



Article

Stability of Blueberry Extracellular Vesicles and Their Gene Regulation Effects in Intestinal Caco-2 Cells

Yangfan Leng ^{1,†}, Liubin Yang ^{1,†}, Hangxin Zhu ¹, Dongqin Li ², Siyi Pan ^{1,3}  and Fang Yuan ^{1,3,*} 

¹ College of Food Science and Technology, Huazhong Agricultural University, Wuhan 430070, China; 593lyfmail.hzau.edu.cn@webmail.hzau.edu.cn (Y.L.); yangliubin@mail.hzau.edu.cn (L.Y.); zh_1@webmail.hzau.edu.cn (H.Z.); pansiyi@mail.hzau.edu.cn (S.P.)

² National Key Laboratory of Crop Genetic Improvement, National Center of Plant Gene Research (Wuhan), Huazhong Agricultural University, Wuhan 430070, China; ldq@mail.hzau.edu.cn

³ Hubei Key Laboratory of Fruit & Vegetable Processing & Quality Control, Huazhong Agricultural University, Wuhan 430070, China

* Correspondence: fyuan@mail.hzau.edu.cn

† These authors contributed equally to this work.

Abstract: Plant extracellular vesicles (P-EVs) are considered promising functional food ingredients due to their various health benefits. In this study, blueberry extracellular vesicles (B-EVs) were collected and purified by size exclusion chromatography (SEC). The chemical compounds in B-EV extracts were analyzed by LC-MS/MS. In addition, the stability of B-EVs was evaluated during short- and long-term storage, heating, and in vitro digestion. The results showed that the B-EVs had a desirable particle size (88.2 ± 7.7 nm). Protein and total RNA concentrations were 582 ± 11.2 $\mu\text{g}/\text{mL}$ and 15.4 $\mu\text{g}/\text{mL}$, respectively. The optimal storage temperatures for B-EVs were 4 °C and -80 °C for short- and long-term storage, respectively. Fluorescent labeling and qRT-PCR tests showed that B-EVs could be specifically internalized by Caco-2 cells, whereas virtually no cytotoxic or growth-inhibitory effects were observed. B-EVs down-regulated the expression levels of *IL-1 β* and *IL-8* and up-regulated the expression levels of *NF- κ B* and *TLR5* in Caco-2 cells. Overall, the results proved that the intact structure of B-EVs could be preserved during food storage and processing conditions. B-EVs had the ability to reach the human intestine through oral delivery. Moreover, they could be absorbed by intestinal cells and affect human intestinal function.

Keywords: blueberry extracellular vesicles; stability; in vitro digestion; storage; LC-MS/MS



Citation: Leng, Y.; Yang, L.; Zhu, H.; Li, D.; Pan, S.; Yuan, F. Stability of Blueberry Extracellular Vesicles and Their Gene Regulation Effects in Intestinal Caco-2 Cells. *Biomolecules* **2023**, *13*, 1412. <https://doi.org/10.3390/biom13091412>

Academic Editor: Lutfun Nahar

Received: 5 September 2023

Revised: 14 September 2023

Accepted: 18 September 2023

Published: 19 September 2023



Copyright: © 2023 by the authors. Licensee MDPI, Basel, Switzerland. This article is an open access article distributed under the terms and conditions of the Creative Commons Attribution (CC BY) license (<https://creativecommons.org/licenses/by/4.0/>).

1. Introduction

Plant extracellular vesicles (P-EVs) are membrane-enclosed vesicles with diameters of 50 nm–300 nm, containing bioactive molecules such as proteins, lipids, and RNAs. Plants excrete P-EVs for cell-to-cell communication, immune system regulation, and defense from pathogen invasions [1]. When the plants are consumed as food, P-EVs can be absorbed by the consumer's intestinal macrophages and induce the expression of multiple cytokines in the host [2]. Among the cargos of P-EVs, microRNAs (miRNAs) have gained a lot of interest because they can regulate gene expression post-transcriptionally and exert multiple health benefits and functionalities [3]. For example, in ginger-derived extracellular vesicles (G-EVs), miRNA mdo-miR7267-3P induced interleukin-22 (IL-22) production to relieve the symptoms of colitis [4]. Another study reported that miR-CM1 derived from *Phellinus linteus* extracellular vesicles can inhibit the expression of *Mical2* to alleviate ultraviolet-induced skin aging [5]. In addition to miRNAs, proteins, lipids, and other chemicals were also reported to be functional components in P-EVs. The heat shock protein (HSPA8) in mulberry bark EVs can activate aryl hydrocarbon receptor (AHR)-mediated signaling in mice to prevent DSS-induced colitis [6]. Chen et al. [7] reported that the lipid of G-EVs can inhibit the assembly and activation of NLRP3 inflammasome to regulate

inflammation. Additionally, strawberry-derived EVs can reduce reactive oxygen species (ROS) due to high vitamin C content [8]. These bioactive molecules can be encapsulated in P-EVs and manage to survive harsh conditions in the circulation of the host [9]. The P-EVs were able to maintain their structures when exposed to the ex vivo digestion process with only changes in size and charge [10]. When given orally, some P-EVs can also survive the digestion process, enter the colon area [10], and be absorbed by intestinal cells via endocytosis and further travel via the bloodstream [11]. However, since P-EVs are different from animal exosomes in many biological aspects, several basic problems are still unsolved. For example, protein markers need to be established and unified. PEVs contain multiple components, such as lipids, proteins, nucleic acids, and secondary metabolites, and their specific substances and mechanisms of action need to be further studied and explored.

Blueberry (*Vaccinium* spp.) has been reported to have multiple health benefits, such as oxidative stress regulation and anti-inflammation [12]. Blueberry extracellular vesicles (B-EVs) were reported to relieve oxidative stress by the positive modulation of HMOX1 and NRF1 in EA. hy926 cells [13]. Zhao et al. [14] also reported that B-EVs can decrease the expression levels of aspartate aminotransferase and alanine aminotransferase to improve insulin resistance and liver dysfunction and attenuate the accumulation of lipid droplets by inhibiting the expression of fatty acid synthase and acetyl-CoA carboxylase. In our recent study, we found that the miRNAs in B-EVs were predicted to target human genes involved in intestinal immune response [15], indicating that B-EVs might be used as a novel functional food ingredient to promote human intestinal health. Adhesion of B-EVs to the intestinal surface is an important property that confers immune system modulation. However, the stability of B-EVs during food processing, storage, and digestion has not been clearly demonstrated yet. Therefore, the objective of this study was to (i) determine the effect of storage conditions, heat treatments, and in vitro simulated gastrointestinal digestion on B-EVs' stability; and (ii) investigate the internalization and gene regulation effects of B-EVs when contacting human intestinal cells.

2. Materials and Methods

2.1. Separation and Identification of B-EVs

Blueberries were purchased from a local market. Blueberries (250 g) with 1000 mL of phosphate-buffered saline solution (PBS) were well mixed using a household juicer, and then the mixture was used for extracting B-EVs according to a previously described method [15]. Briefly, the blueberry juice was centrifuged at $3000 \times g$ for 10 min, $8000 \times g$ for 30 min, and $10,000 \times g$ for 60 min at 4 °C. The supernatant was passed through a 0.22 µm filter and concentrated with a 10,000 MWCO membrane (Millipore, Shanghai, China). Finally, 10 mL of concentrated blueberry juice was added to a commercial qEV 10 column (Izon Science, Canterbury, New Zealand), and the 10 mL eluate was collected as fraction 1. Then 21.4 mL of PBS was loaded and collected as fraction 2. According to our previous research, the B-EVs were abundant in fraction 2 [15]. So fraction 2 was collected and concentrated to around 200 µL with a 10,000 MWCO membrane. The total protein concentration of B-EV isolates was determined using the BCA protein assay kit (Nanjing Jiancheng Bioengineering Institute, Nanjing, China).

The sizes of B-EVs were determined by dynamic light scattering (DLS) using a Zeta-sizer Nano-ZS 90 size analyzer (Malvern Instruments Ltd., Malvern, UK) at 25 °C [15]. The distribution of hydrodynamic diameter, D_h , was determined by using the Stokes–Einstein relationship $D_h = K_B T / 3\pi\eta D_0$, where K_B is the Boltzmann constant, T the absolute temperature, and η the solvent viscosity.

The morphology analysis of B-EVs was carried out by transmission electron microscopy (TEM). TEM analysis was performed following the published method with minor modifications [16]. The B-EVs were added to copper grids at room temperature. Then negative staining was applied to B-EVs for 30 s, using 1% aqueous phosphotungstic acid (PTA) solution (pH 6.4–7), which was positioned at room temperature until the PTA solution was dried completely. Measurements were carried out by using an FEI TECNAI 12 G2

Twin, operating at 80 kV and equipped with an electron energy loss filter and a slow-scan charge-coupled device camera (Hitachi, Tokyo, Japan).

The concentrated blueberry juice and B-EVs were analyzed using LC-MS/MS in positive ESI ionization mode. A Waters Vion IMS Qtof system was equipped with a Waters C18 column (XBridge[®] C18 3.5 μm , 3.0 \times 150 mm). The mobile phases were 0.1% formic acid in water (solvent A) and acetonitrile (solvent B). The gradient was 0–4 min to 100% B; 42–48 min to 5% B; and 48–51 min to 100% B. The mass spectrometer was operated with the following operating parameters: capillary voltage, 3.5 kV; column temperature, 25 $^{\circ}\text{C}$; and velocity of flow, 300 $\mu\text{L}/\text{min}$. The source temperature was 120 $^{\circ}\text{C}$ and the desolvation temperature was 400 $^{\circ}\text{C}$. The desolvation gas flow was 400 L/h. LC-MS/MS analysis follows similar steps as those outlined by Kyung et al. [17].

RNAs from B-EVs were extracted with an Easstep[®] Super Total RNA Extraction Kit (Promega Co., Madison, WI, USA) according to the manufacturer's instructions. Total RNA was collected and the concentration was measured by Qubit 3 Fluorometer (Invitrogen, Carlsbad, CA, USA).

2.2. Stability of B-EVs under Heat Treatments

The extracted B-EVs were subjected to two different heat treatments that may simulate pasteurization during food manufacturing. Half of the sample was heated at 60 $^{\circ}\text{C}$ for 30 min, while the other half was heated at 75 $^{\circ}\text{C}$ for 15 s. The stability of B-EVs under heat treatments was evaluated according to changes in size, morphological features, and total protein, as described in 2.1. Each sample was assayed in triplicate.

2.3. Stability of B-EVs during Storage

The B-EV samples were divided into four groups with three replicates. Then the four groups were stored at -80°C , -20°C , 4°C , and 25°C for 7 d and 30 d, respectively. The stability of B-EVs was evaluated by measuring their size and morphological features using the method described above.

2.4. Stability of B-EVs in Simulated Gastrointestinal Tract Environment

In vitro stability tests were performed according to the published method with minor modifications [10]. Totals of 1.34 μL of 18.5% (*w/v*) HCl (pH 2.0) and 24 μL of pepsin solution (80 mg/mL in 0.1 mol/L HCl, pH 2.0) were added to 1 mL (1 mg/mL) of B-EVs in PBS, and the mixture was incubated at 37 $^{\circ}\text{C}$ for 0.5 h (stomach-like conditions). Then, 80 μL of a mixture containing 24 mg/mL of bile extract and 4 mg/mL of pancreatin in 0.1 N NaHCO_3 was added. The pH was adjusted to 6.5 with 1 N NaHCO_3 and incubated for an additional 0.5 h at 37 $^{\circ}\text{C}$ (intestine-like conditions). The stability of B-EVs was evaluated by measuring their size and morphological features using the method described above.

2.5. Caco-2 Cell Culture

The human Caco-2 intestinal epithelial cell line was purchased from Procell (Wuhan, China). The culture medium contained 89% Dulbecco's Modified Eagle Medium (DMEM, GIBCO, Shanghai, China), 10% fetal bovine serum (FBS, GIBCO, China), and 1% penicillin-streptomycin (Biosharp, Hefei, China). Cells were cultured in a T75 culture flask (Thermo Scientific[™], Shanghai, China) and incubated in a carbon dioxide incubator at 37 $^{\circ}\text{C}$ and 5% CO_2 . An inverted microscope (Nikon Ti-S, Tokyo, Japan) was used to observe cell adhesion and growth. The culture medium was changed every 24 h. Cell transmission follows the same steps as described in Bruno et al. [18].

2.6. Cytotoxicity Assay

A cytotoxicity assay was performed according to the published method with minor modifications [18]. Caco-2 cells were seeded in three 96-well plates at a density of 1×10^4 cells/well with 100 μL of culture medium and incubated for 4–6 h to promote cell adhesion to the wall. B-EV concentration was expressed as the concentration of protein

in the extract. Additionally, the concentration gradient was determined after a careful review of previous publications [8,18,19]. Adherent cells were then treated with 10 μ L of culture medium mixed with different concentrations of B-EVs (0, 5, 10, 20 μ g/mL, with 7 repetitions per group) and incubated for 12 h, 24 h, and 36 h. At each time point, the B-EV-containing medium was removed and cells were thoroughly rinsed twice with PBS. Then, 100 μ L of fresh, non-supplemented DMEM and 10 μ L of CCK8 (Beyotime, Shanghai, China) were added in each well. After 1 h incubation, absorption was measured by a Multiskan GO microplate reader (Thermo, Waltham, MA, USA) at a wavelength of 450 nm. Student's *t*-test was used to analyze cell cytotoxicity at different times and concentrations.

2.7. Preparation of Caco-2 Monolayers

Caco-2 cells were seeded onto polycarbonate filters inside Transwell cell culture chambers (Servicebio, Wuhan, China) at a density of 2×10^5 cells/cm². The culture medium was added to the chamber (0.5 mL in the insert and 1.5 mL in the well). The transepithelial electric resistance (TEER) of the monolayers was checked using an electrical resistance system (Millicell, Shanghai, China). The culture medium changing and transmission followed the same protocols as those described by Saliba et al. [20] A TEER value higher than 500 Ohm·cm² indicates that the cells have fully differentiated [21].

2.8. B-EV Labeling

Fluorescent labeling of B-EVs was carried out using the pKH26 Fluorescent Cell Ligation Kit (Solarbio, Beijing, China) according to the manufacturer's instructions. Briefly, equal volumes of samples were mixed with dye and incubated at 37 °C for 30 min. Subsequently, 1 \times PBS was added and the sample was centrifuged for 1 h at 120,000 \times *g*, repeating three times to remove the unbound-free dye. Labeled B-EVs were resuspended in DMEM for further experiments.

2.9. In Vitro Internalization of B-EVs by Caco-2 Cells

Labeled B-EVs were incubated with fully differentiated Caco-2 cells for 6 h, 12 h, and 24 h. After incubation, cells were fixed with 4% paraformaldehyde (PFA) for 10 min. Then DAPI (Beyotime, Shanghai, China) and DIO (Beyotime, Shanghai, China) were added to label the cell nucleus and cell membranes, respectively. Finally, cells were coverslip-mounted and a confocal laser scanning microscope (Olympus FV3000, Tokyo, Japan) was used to capture the images. The excitation wavelengths of DIO, PKH26, and DAPI were 484 nm, 340 nm, and 551 nm, respectively. Additionally, to explore the mechanisms associated with B-EV absorption, the endocytosis inhibitor (Chlorpromazine) was preincubated with Caco-2 cells for 1 h. The labeled B-EVs were added to fully differentiated Caco-2 cells and incubated for another 24 h at 37 °C. Caco-2 cells were seeded onto 12-well plates and were incubated with B-EVs for 24 h. Cells without B-EVs were used as a negative control.

2.10. Quantitative Real-Time Polymerase Chain Reaction (qRT-PCR)

After incubation, the total RNA of Caco-2 cells was extracted using the phenol-chloroform method. First-strand cDNA was synthesized by using the SweScript All-in-One First-Strand cDNA Synthesis SuperMix Kit (One-Step gDNA Remover) (Wuhan Servicebio Technology Co., Ltd., Wuhan, China). The first-strand cDNA mix was prepared by combining 4 μ L of 5 \times SweScript All-in-One SuperMix Kit for qPCR, 1 μ g of total RNA, and 1 μ L of gDNA remover, and then nuclease-free water was added for a final volume of 20 μ L. The GAPDH gene was used as a control and specific primers were designed based on cDNA sequences (Table S1). Real-time PCR was performed with the following program: 95 °C for 30 s, followed by 40 cycles at 95 °C for 15 s, 60 °C for 10 s, and 72 min for 3. Relative gene expression was calculated using the Livak and Schmittgen $2^{-\Delta\Delta C_t}$ method [22], normalized with the reference gene GAPDH. QPCR amplifications were performed in triplicate for each sample. The data were examined by *t*-test.

2.11. Statistical Analysis

Statistical analysis was performed using SPSS 22.0 (SPSS, Chicago, IL, USA). All data were representative of three independent experiments and statistical differences were considered significant at * $p < 0.05$ or ** $p < 0.01$. Image processing was performed using Origin Pro 2019b (Origin Lab Corporation, Northampton, MA, USA).

3. Results

3.1. Characterizations of B-EVs Obtained via SEC Methods

Size exclusion chromatography (SEC) is becoming a widely used technique to extract and purify P-EVs using simple steps. In this study, SEC was used to extract the EVs derived from blueberries. SEC performed well in removing the anthocyanins in the blueberry, as the color of the solution changed from purple to transparent after SEC extraction (Figure 1A). The results showed that B-EVs extracted by SEC had a round shape with a clear membrane structure (Figure 1B), desirable particle size (88.2 ± 7.7 nm), and a low PDI (0.19 ± 0.02) (Figure 1C and Table S2). The B-EV extract had 482.2 ± 11.2 $\mu\text{g}/\text{mL}$ of protein and 15.4 $\mu\text{g}/\text{mL}$ of RNA. Compared with other studies, the SEC method was more effective in removing protein contaminants of P-EVs (Table S3). Additionally, LC-MS/MS was used to compare the compound in the centrifuged blueberry juice (before SEC) and in the B-EVs extract. As presented in Table 1, before SEC, the centrifuged blueberry juice was enriched with polyphenols, flavonoids, and anthocyanins (Figure S1). However, only 6-O-Malonylgenistin was detected in the B-EV extract purified by SEC, and the peak area was reduced by about 50%.

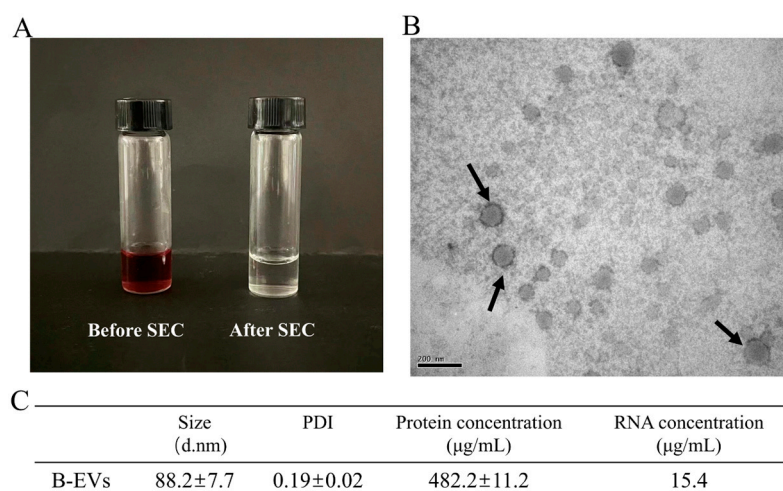


Figure 1. Characterization of B-EVs extracted by SEC. (A) A picture of centrifuged blueberry juice (before SEC) and B-EVs. (B) TEM image of B-EVs isolated via SEC. (C) The size, total protein concentration, and RNA concentration of B-EVs.

Table 1. Compounds identified in centrifuged Blueberry juice (before SEC) and in the B-EV extract via LC-MS/MS.

| No. | Compounds | Molecular Formula | RT (min) | Precursor (m/z) | MS/MS (m/z) | Response (Centrifuged Blueberry Juice) | Response (B-EV Extract) |
|-----|---|---|----------|-----------------|-------------|--|-------------------------|
| 1 | 3-O-Methylgallic acid | $\text{C}_8\text{H}_8\text{O}_5$ | 5.16 | 185.0429 | 142.00346 | 942.3 ± 54.5 | ND |
| 2 | Coumarin | $\text{C}_9\text{H}_6\text{O}_2$ | 5.34 | 147.044 | 102.96836 | 2783.0 ± 334.0 | ND |
| 3 | Malvidin | $\text{C}_{23}\text{H}_{25}\text{O}_{12}$ | 48.15 | 493.1339 | 332.08495 | $32,490.7 \pm 4927.0$ | ND |
| 4 | 3-O- β -D-galactoside Isopeonidin | $\text{C}_{21}\text{H}_{21}\text{O}_{10}$ | 49.48 | 433.1124 | 270.02277 | 2921.3 ± 1644.1 | ND |
| 5 | 3-O-arabinoside Malvidin 3-arabinosid | $\text{C}_{22}\text{H}_{23}\text{O}_{11}$ | 49.59 | 463.1234 | 301.06164 | $17,968.0 \pm 6999.2$ | ND |

Table 1. Cont.

| No. | Compounds | Molecular Formula | RT (min) | Precursor (m/z) | MS/MS (m/z) | Response (Centrifuged Blueberry Juice) | Response (B-EV Extract) |
|-----|------------------------------------|---|----------|-----------------|-------------|--|-------------------------|
| 6 | 5,6,7,3',4'-Pentahydroxyisoflavone | C ₁₅ H ₁₀ O ₇ | 50.35 | 303.0492 | 257.04602 | 10,522.0 ± 2943.6 | ND |
| 7 | Petunidin-glucoside | C ₂₂ H ₂₃ O ₁₂ | 50.37 | 479.1192 | 317.06595 | 1748 ± 301 | ND |
| 8 | Luteolin | C ₁₅ H ₁₀ O ₆ | 50.47 | 287.0546 | 133.12206 | 950.7 ± 133.4 | ND |
| 9 | 6-O-Malonylgenistin | C ₂₄ H ₂₂ O ₁₃ | 51.18 | 519.1139 | 270.44986 | 8657.1 ± 1025.8 | 4340 ± 660.1 |

3.2. Stability of B-EVs under Heat Treatments

The stability of B-EVs was first evaluated under two different heat treatment conditions (60 °C for 30 min and 75 °C for 15 s) that mimic traditional pasteurization. After heat treatments, the size distribution, morphology, and protein content of B-EVs were measured and compared with non-treated B-EVs (Control) (Figure 2A). Transmission electron microscopy (TEM) showed that the B-EVs were cup-shaped with a clear membrane structure. Dynamic light scattering (DLS) showed that the freshly extracted B-EVs had an asymmetric size distribution of 50 nm to 220 nm, with an average size of 87.6 nm. After heating at 60 °C for 30 min and at 75 °C for 15 s, the average diameter of B-EVs increased 35% and 33%, respectively. Heat treatments lowered the total protein content in the B-EV extract. Both heat treatments changed the B-EVs' morphology, as part of the flat cup-shaped vesicles turned into polygon-shaped vesicles, and more aggregates were observed.

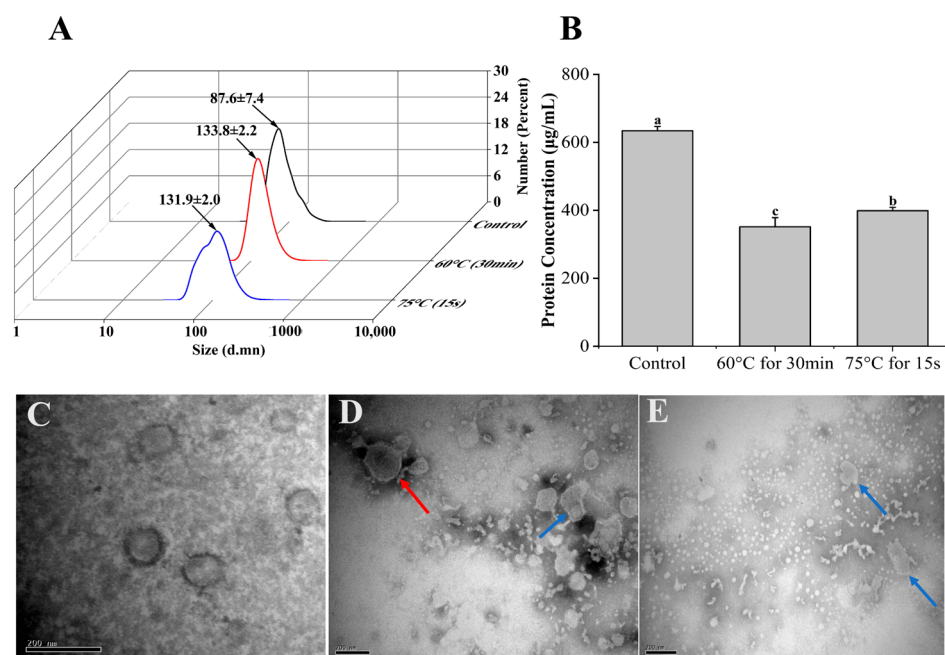


Figure 2. Stability of B-EVs in a simulated food processing environment. (A) Size distribution of B-EVs from two heat treatments (60 °C for 30 min; 75 °C for 15 s). The black arrows represent the mean of the main peak of B-EVs; (B) protein concentration of B-EVs after heat treatments. Different letters in the column chart represent significantly (Tukey HSD, $p < 0.05$) different in means; (C) TEM image of freshly extracted B-EVs; (D) TEM image of B-EVs heated at 60 °C for 30 min; (E) TEM image of B-EVs heated at 75 °C for 15 s. The red arrows represent aggregated B-EVs and the blue arrows show morphologically changed B-EVs. Data are represented as mean ± standard error. scale bar: 20 nm.

3.3. Stability of B-EVs during Storage

B-EVs were stored at four different temperatures (−80 °C, −20 °C, 4 °C, and 25 °C) for 7 days and 30 days, respectively (Figure 3). However, since the storage of B-EVs at 25 °C

for 30 days led to severe microbial growth, the data were discarded. Freezing storage is the most commonly used storage condition for P-EVs, but our results showed that freezing conditions resulted in morphological changes to B-EVs. B-EVs stored at $-80\text{ }^{\circ}\text{C}$ and $-20\text{ }^{\circ}\text{C}$ for 7 days were larger in size (they increased by 34% and 49%, respectively) compared to freshly isolated B-EVs, and some larger nanovesicle aggregates of up to 300 nm in diameter were generated after freezing for 7 days. TEM observation also showed that after freezing, B-EVs were becoming larger and more aggregated, and had more multi-lamellar membrane layers (Figure 3E,F). For the long-term storage (30 days), DLS data also showed that the size of B-EVs increased. After 30 days of storage at $-80\text{ }^{\circ}\text{C}$ and $-20\text{ }^{\circ}\text{C}$, the average diameter increased 28% and 48%, respectively, compared to the control (Figure 3B,I). The protein content decreased in comparison to the control, regardless of short-term or long-term preservation (Figure 3C).

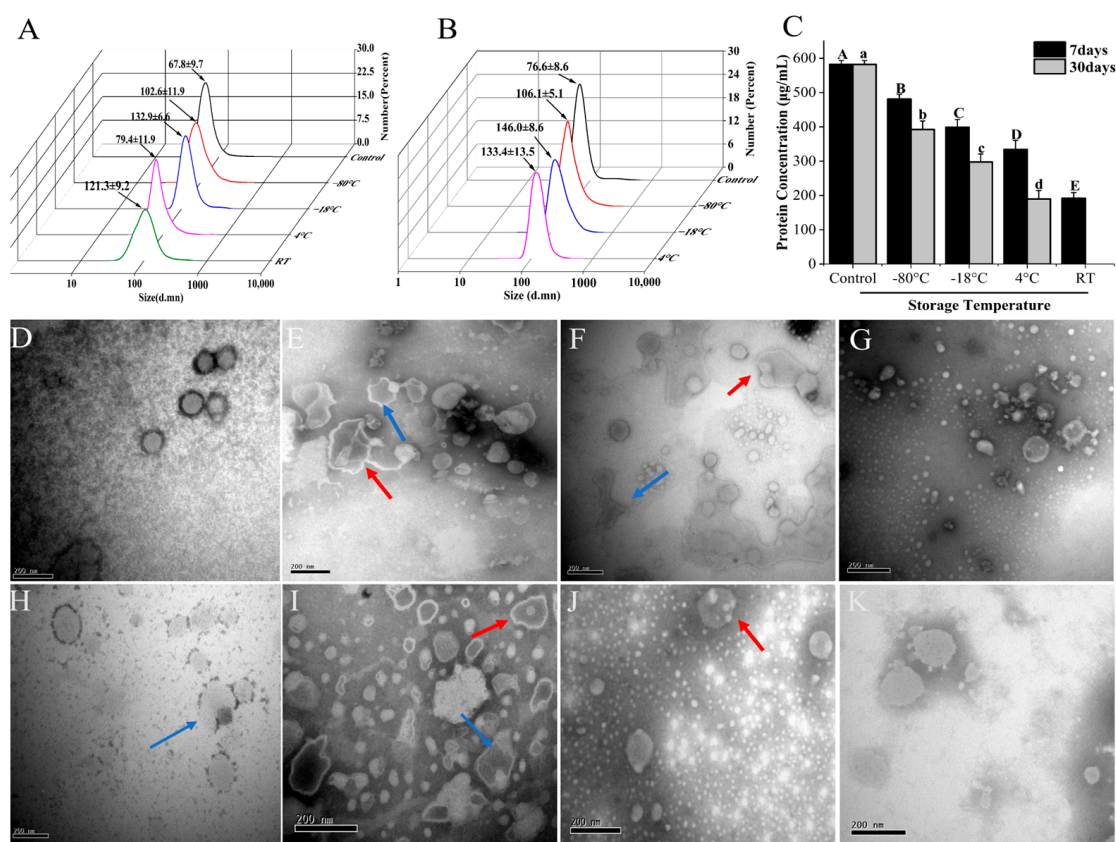


Figure 3. Stability of B-EVs under various storage temperatures. (A) Particle sizes of B-EVs stored at $-80\text{ }^{\circ}\text{C}$, $-18\text{ }^{\circ}\text{C}$, $4\text{ }^{\circ}\text{C}$, and $25\text{ }^{\circ}\text{C}$ for 7 days; (B) particle sizes of B-EVs stored at $-80\text{ }^{\circ}\text{C}$, $-18\text{ }^{\circ}\text{C}$, and $4\text{ }^{\circ}\text{C}$ for 30 days; (C) protein concentration of B-EVs under various storage temperatures. Different letters in the column chart represent significantly (Tukey HSD, $p < 0.05$) different in means; TEM images of B-EVs stored for 7 days: control (D), $-80\text{ }^{\circ}\text{C}$ (E), $-18\text{ }^{\circ}\text{C}$ (F), $4\text{ }^{\circ}\text{C}$ (G), and $25\text{ }^{\circ}\text{C}$ (H); TEM images of B-EVs stored for 30 days: $-80\text{ }^{\circ}\text{C}$ (I), $-18\text{ }^{\circ}\text{C}$ (J), $4\text{ }^{\circ}\text{C}$ (K). The red arrows represent aggregated B-EVs and the blue arrows show morphologically changed B-EVs. Data are represented as mean \pm standard error. scale bar: 20 nm.

Since refrigerator and room temperature storage are also common for fruits and fruit juice, we tested the stability of B-EVs at $4\text{ }^{\circ}\text{C}$ and $25\text{ }^{\circ}\text{C}$. The size and shape of B-EVs stored at $4\text{ }^{\circ}\text{C}$ for 7 days were similar in comparison to the control (Figure 3G). But after 30 days, the B-EVs showed full or partial degradation (Figure 3K). The size of B-EVs increased 44% when stored at $25\text{ }^{\circ}\text{C}$ for 7 days. It was observed that the membrane structure of some B-EVs became discontinuous (Figure 3H).

3.4. Stability of B-EVs in *In Vitro* Digestion Conditions

The average dimension of B-EVs incubated in the gastric (GS) solution enlarged from 85.5 nm to 100.8 nm (Figure 4A). But B-EVs in the following enteric phase (EP) solution showed a significant decrease compared with B-EVs in the GS solution (from 100.8 ± 7.9 nm to 83.4 ± 4.6 nm). The total protein content had a dramatic increase due to the addition of enzymes in simulated gastrointestinal processing. TEM showed that the B-EVs aggregated after treatment with the GS solution, which was highly correlated with the DLS result with respect to the size of B-EVs increasing (Figure 4C). TEM results also showed that the sizes and shapes of most B-EVs were preserved. The membranes of B-EVs were degraded into smaller pieces when B-EVs were incubated in the EP solution (Figure 4D).

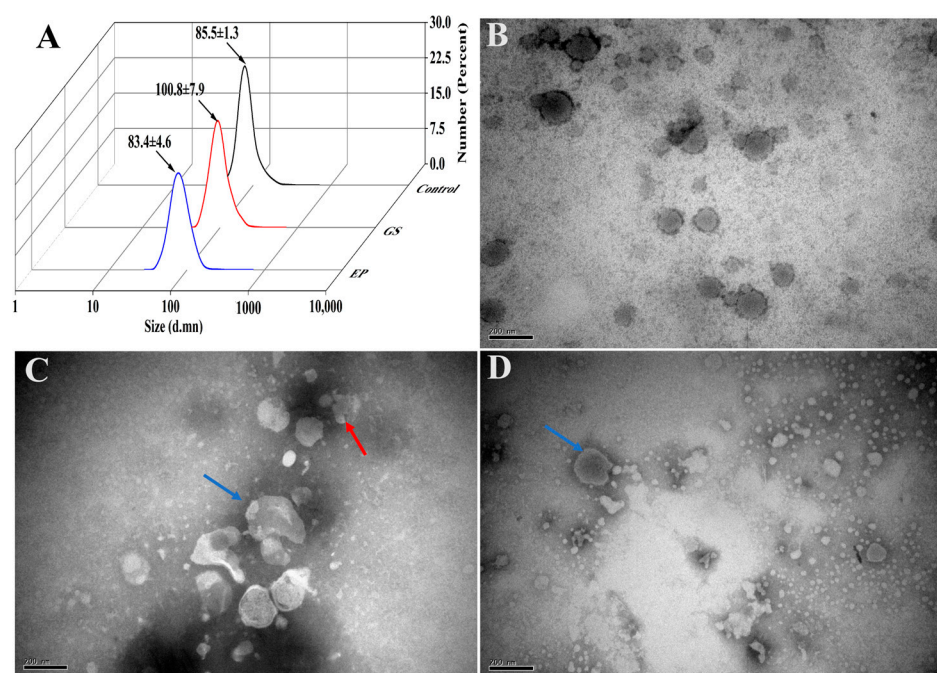


Figure 4. Stability of B-EVs in a simulated gastrointestinal tract environment. (A) The sizes of B-EVs before treatment (control), after treatment with GS (GS), and after treatment with GS followed by an EP solution (EP); (B) TEM image of freshly extracted B-EVs; (C) TEM image of B-EVs in simulated GS solution; (D) TEM image of B-EVs in simulated EP. The red arrows represent aggregated B-EVs and the blue arrows show morphologically changed B-EVs. scale bar: 20 nm.

3.5. Cytotoxicity of B-EVs against Caco-2 Cells

B-EVs were co-cultured with Caco-2 cells for 12 h, 24 h, and 36 h, respectively. No statistical differences were observed between different B-EV treatments and the control group, indicating that B-EVs were not cytotoxic to Caco-2 cells (Figure 5).

3.6. Uptake and Transepithelial Transport of B-EVs across Intestinal Epithelium *In Vitro*

To monitor the dynamic process of B-EV absorption, Caco-2 cells were exposed to PKH26-labeled B-EVs with red fluorescence for 6 h, 12 h, and 24 h. As shown in Figure 5, there was no red fluorescence inside the cells at 6 h. After 12 h of incubation, a few red spots were distributed between the nucleus (blue) and the cell membrane (green) of the Caco-2 cells, indicating that the B-EVs began to be internalized. And after 24 h, a large number of red spots were concentrated around the blue nucleus of the Caco-2 cells, implying that B-EVs had completely entered Caco-2 cells. Confocal analysis showed that when the Caco-2 cells were pre-treated with chlorpromazine, no red vesicles were observed in the Caco-2 cells (Figure 6).

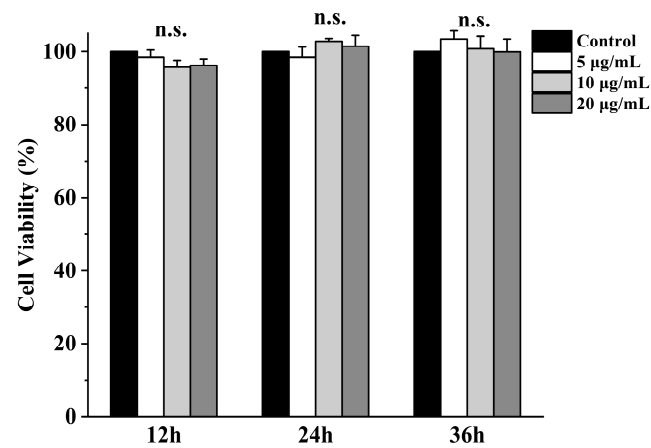


Figure 5. Viability of Caco-2 cells after B-EV treatment. Cell viability was assessed by MTT assay at 12 h, 24 h, and 36 h after incubation with 5, 10, and 20 µg/mL B-EVs, respectively. “n.s.” means no significance.

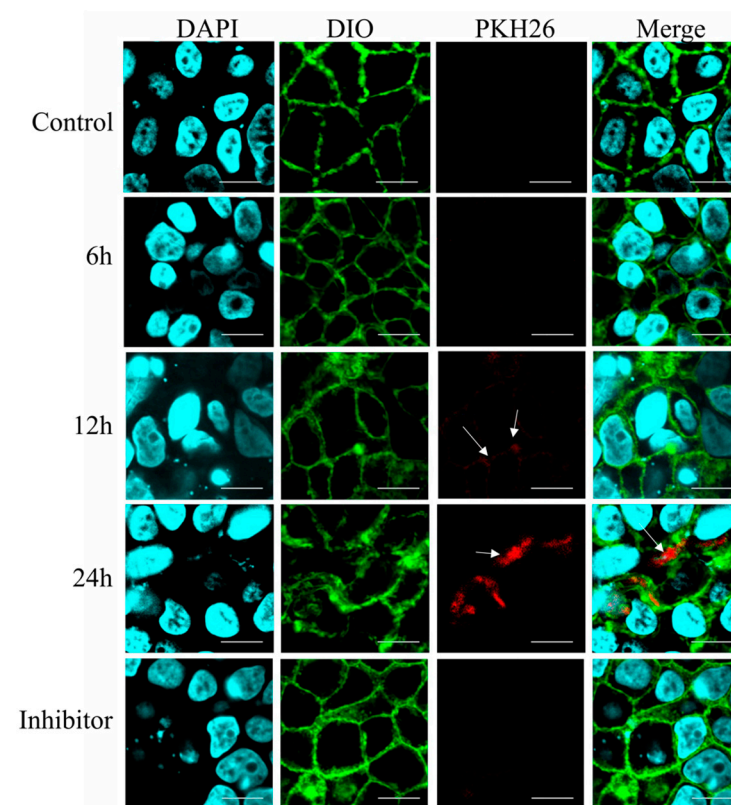


Figure 6. Fluorescence microscopy images of Caco-2 cells incubated with the PKH26-labeled B-EVs for 6 h, 12 h, and 24 h. Inhibitor: Caco-2 cells were pretreated with chlorpromazine for 30 min and then incubated with B-EVs. Caco-2 cell nuclei were labeled with DAPI (blue); the Caco-2 cell membrane was labeled with DIO (green); and B-EVs were labeled with PKH26 (red). The white arrows showed the PKH26-labeled B-EVs.

3.7. Effect of B-EVs on Inflammatory Response in the Intestinal Epithelium Cells

According to the confocal results, B-EVs were completely internalized after 24 h of co-culturing. So we speculated that after 24 h, the effect of B-EVs on inflammatory response would be obvious. Hence, B-EVs and Caco-2 cells were co-cultured for 24 h and the changes in gene expression were measured using quantitative real-time PCR (qRT-PCR). Ten inflammatory-related genes were selected according to the literature and predicted target genes for miRNA of B-EVs [15]. Four out of the ten genes had a significant expression

change. The results showed that B-EVs down-regulated the gene expression levels of interleukin 1 β (*IL-1 β*) and interleukin 8 (*IL-8*), whereas the nuclear factor kappa-light-chain-enhancer of activated B cells (*NF- κ β*) and toll-like receptor 5 (*TLR5*) gene expression levels were up-regulated compared to the control group (Figure 7).

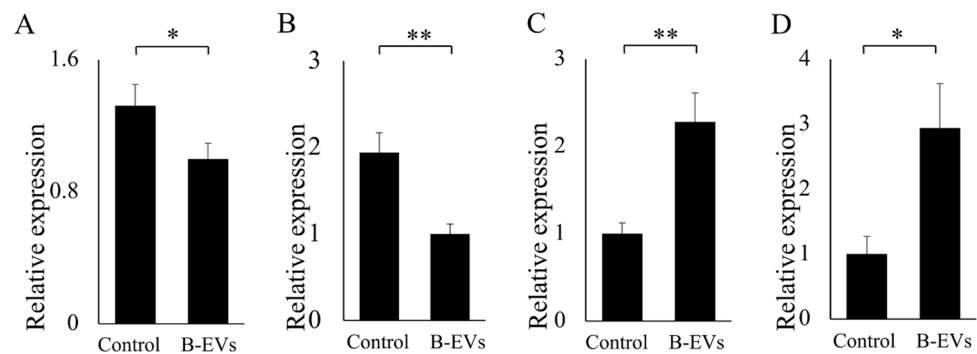


Figure 7. Effect of B-EVs on the relative expression of genes related to inflammation. (A) *IL-1 β* ; (B) *IL-8*; (C) *TLR5*; (D) *NF- κ β* . Statistical significance is indicated as * for $p < 0.05$ and ** for $p < 0.01$.

4. Discussion

Multiple studies have shown that edible P-EVs have various health benefits for consumers. However, the stability of P-EVs under heat treatments and storage conditions is important to evaluate in terms of their suitability to serve as novel functional food ingredients. Our results showed that B-EVs could maintain their structural integrity at pasteurization temperatures, speculating that some bioactive components of B-EVs, such as miRNA and proteins, were able to access the human intestine because of the encapsulated capability of B-EVs. Our result was similar to the report of Li et al. [23], which suggested that EVs could be found in traditional Chinese medicine boiled with water for 30 min, and lipids, small molecule metabolites, proteins, and sRNAs could also be detected after boiling. EVs were also found in cooked pork [24] and roasted hot coffee beverages [25], indicating that, although they were from different sources, EVs generally had a good resistance to heat treatments. Some studies suggested that the interaction between endogenous miRNAs and exosomes might promote the stability of miRNAs during heat treatment [25,26]. However, other studies suggested that whether the stability of miRNAs in cooked or processed food was solely due to encapsulation by P-EVs still needed further investigation [11], since many sRNAs in *Arabidopsis* leaf EVs were more likely to be associated with proteins outside the membranes instead of being fully encapsulated inside EVs [27].

Storage is a crucial factor that influences the physical properties and functionality of P-EVs. Surprisingly little is known about which condition is the most suitable for the storage of P-EVs. Although the stability of extracted EVs from mammals has been examined by accumulated studies, there remains some controversy about the influence of different storage temperatures on EVs. The majority of studies have suggested that mammal-derived EVs be stored at $-80\text{ }^{\circ}\text{C}$ [28,29]. Additionally, it seems to be commonly recognized that P-EVs should also be preserved at $-80\text{ }^{\circ}\text{C}$ [30]. In this study, we observed the particle size increase and morphological changes of B-EVs during storage at different temperatures. Although $-80\text{ }^{\circ}\text{C}$ storage could maintain the particle size of B-EVs, freezing resulted in more “vesicles in vesicle” shaped B-EVs, with some vesicles being dense and others seeming to be empty. This phenomenon could be explained, in part, by the phospholipid bilayer membrane of B-EVs possibly being damaged by ice crystals during freezing, and these crystals producing the de-mixing of biological surfactants, resulting in a fusion between miscible membranes during dehydration and shaping of the multilamellar vesicles [31]. When compared to $-80\text{ }^{\circ}\text{C}$, B-EVs stored at $4\text{ }^{\circ}\text{C}$ for 7 days were still round shaped with a clear membrane structure. Considering storage at $-80\text{ }^{\circ}\text{C}$ is prohibitively costly, $4\text{ }^{\circ}\text{C}$ storage of B-EVs is an alternative way to preserve B-EVs in the short term, which is consistent with the results of previous reports that HEK 293 T cell-derived EVs stored at

4 °C or 37 °C for 24 h were better than those stored at freezing temperatures [32]. However, as the storage time increased to 30 days, B-EVs started to swell, and the membrane degraded quickly as the temperature increased. So for long-term storage, it is still recommended to store B-EVs at −80 °C. Additionally, it is worth mentioning that, in our experience, a repeated freeze–thaw cycle may cause significant damage to B-EVs because of the fragility of phosphatidylserine on the lipid bilayer of B-EVs when exposed to ice crystals [33].

The stability of B-EVs in human digestive systems should be clearly demonstrated before B-EVs could be utilized as functional food ingredients. Our study showed that the microstructures of some B-EVs were altered after incubation in simulated gastrointestinal fluids. Extensive particle aggregation was observed in simulated gastric fluids, and some of the large aggregates formed in the GS solution then broke down into smaller clumps after exposure to the EP solution. This might be caused by partial hydrolysis of B-EVs by enzymes or by changes in electrostatic interactions caused by alterations in ionic strength and pH. The stability of P-EVs from other plant species has been tested in the human digestive system, but the results are still subject to debate. Reports of P-EV size changes during the digestive process were prevalent. Similar to our observation, the size of oat-derived EVs increased in a stomach-like solution and then decreased in a small-intestine-like solution [34]. However, another study suggested that the sizes of citrus-derived EVs were not changed after passing through the gastric solution, but increased in the intestinal solution. [18] The size of ginger-derived EVs was reduced slightly in a simulated gastrointestinal tract environment [10]. In contrast, other research showed that tartary buckwheat-derived EVs had no obvious change in their particle size and zeta potential during passage through a simulated gastrointestinal tract [35]. These results indicated that EVs from different plant species might have different abilities to resist gastrointestinal digestion. In addition, other particles in P-EV extracts, such as proteins and cell debris, could also affect the size measurement results. So different extraction and purification methods for P-EVs should also be considered.

The Caco-2 cell line is derived from human intestinal epithelium and is a widely accepted in vitro model for studying cytotoxicity and delivery [20]. Our results showed that B-EVs were non-toxic and harmless to Caco-2 cells. The result is consistent with many studies supporting that EVs derived from edible plants are nontoxic. For example, the concentration gradient of strawberry EVs was from 2 to 9 µg/mL, confirming that strawberry EVs did not exert any significant toxic effect on the adipose-derived mesenchymal stem cells [8]. Citrus EVs and pomegranate EVs did not significantly alter the cell viability of Caco-2 cells [19]. The cytotoxicity of plant-derived EVs was low, probably because P-EVs were composed of natural origin cellular components and derived from plants. Our results also suggested that B-EVs could be easily internalized by Caco-2 cells via endocytosis and distributed throughout the host cytoplasm after endocytosis. Similar results in terms of intracellular distribution were also reported in other research [18,36]. After being internalized by Caco-2 cells, B-EVs modulated the expression of important genes related to inflammatory pathways in the Caco-2 cells, such as *IL-1β*, *IL-8*, *TLR5*, and *NF-κβ*, to affect intestinal inflammation [37]. Among them, *NF-κβ* was a central player in the signaling cascades mediating inflammation. Another study reported that the production of *NF-κβ*, cytokines, and chemokines via the triggering of toll-like receptor 4 (*TLR4*) could activate endogenous immunity, which is beneficial to the organism to a certain extent [38]. Previous studies suggested that EVs were effective vehicles for transferring plant-derived miRNAs to mammalian cells. Additionally, plant miRNAs have shown targeting effects on mammalian gene expression both in vivo and in vitro [18,31]. Our previous research also found that *TLR 5* was the predicted target gene for the miR-466i of B-EVs. In this study, we inferred that B-EVs were effective delivery systems, and the abundant microRNA within EVs may play regulatory roles in the expression of immune-related genes. Incontestably, there were still a few unavoidable contaminants in the B-EV extracts, such as proteins and anthocyanins, which might also play a regulatory role. P-EVs utilize proteins to carry out diverse cellular functions and facilitate intercellular communication by transferring their

cargo to recipient cells, resulting in antioxidant stress reduction and anti-inflammatory activation [39,40]. Further research is needed to comprehensively identify the wide range of P-EV proteins involved in their biological and pharmacological activities. Our results indicated that B-EVs regulated some genes in Caco-2 cells, but the downstream bioprocess of these changes is not clear. More *ex vivo* studies are still needed to explore the role of B-EVs as a food component in regulating human intestinal health.

5. Conclusions

This study proposed effective storage conditions for B-EVs: 4 °C for short-term storage and −80 °C for long-term storage. The 4 °C storage could prevent the ice crystals from damaging the phospholipid bilayer membrane of B-EVs, while −80 °C could slow down the degradation rate. B-EVs had certain stability in simulated gastrointestinal and processing environments. In addition, B-EVs were not cytotoxic and could be easily internalized by intestinal epithelium cells, regulating the host inflammation response. These results provided a theoretical basis for blueberry-derived EVs as a novel functional food ingredient. It is worth mentioning that there is still a lack of a one-size-fits-all solution for the storage of P-EVs. Further research is still needed to obtain B-EVs with higher efficiency and higher purity, which could be helpful in verifying the effect of B-EVs *in vivo*.

Supplementary Materials: The following supporting information can be downloaded at: <https://www.mdpi.com/article/10.3390/biom13091412/s1>. Table S1. Primer Sequences Used for Quantitative RT-PCR. Table S2. Polydispersity Indexes of B-EVs under various conditions. Table S3. Comparison of the protein concentrations in EVs isolated from different sources. Figure S1. (A) The total ion chromatogram of centrifuged blueberry juice (before SEC). (B) The total ion chromatogram of B-EVs. Mass spectrogram of 3-O-Methylgallic acid (C), Coumarin (D), Malvidin 3-O-β-D-galactoside (E), Isopeonidin 3-O-arabinoside (F), Malvidin 3-arabinosid (G), 5,6,7,3',4'-Pentahydroxyisoflavone (H), Petunidin- glucoside (I), Luteolin (J), 6-O-Malonylgenistin (K). References [41–43] are cited in Supplementary Materials.

Author Contributions: Y.L.: conceptualization, methodology, software, writing—original draft, and writing—review and editing. L.Y.: supervision and writing—review and editing. H.Z.: software. D.L.: investigation. S.P.: supervision. F.Y.: supervision and funding acquisition. All authors have read and agreed to the published version of the manuscript.

Funding: This work was supported by the National Natural Science Foundation of China (grant number 31701561).

Data Availability Statement: Data will be made available on request.

Conflicts of Interest: The authors declare no conflict of interest.

References

1. Yi, Q.; Xu, Z.; Thakur, A.; Zhang, K.; Liang, Q.; Liu, Y.; Yan, Y. Current understanding of plant-derived exosome-like nanoparticles in regulating the inflammatory response and immune system microenvironment. *Pharmacol. Res.* **2023**, *190*, 106733. [CrossRef]
2. Suharta, S.; Barlian, A.; Hidajah, A.C.; Notobroto, H.B.; Ana, I.D.; Indariani, S.; Wungu, T.D.K.; Wijaya, C.H. Plant-derived exosome-like nanoparticles: A concise review on its extraction methods, content, bioactivities, and potential as functional food ingredient. *J. Food Sci.* **2021**, *86*, 2838–2850. [CrossRef]
3. Lukasik, A.; Zielenkiewicz, P. Plant microRNAs—Novel players in natural medicine? *Int. J. Mol. Sci.* **2016**, *18*, 9. [CrossRef]
4. Teng, Y.; Ren, Y.; Sayed, M.; Hu, X.; Lei, C.; Kumar, A.; Hutchins, E.; Mu, J.; Deng, Z.; Luo, C. Plant-derived exosomal microRNAs shape the gut microbiota. *Cell Host Microbe* **2018**, *24*, 637–652.e638. [CrossRef] [PubMed]
5. Han, J.; Wu, T.; Jin, J.; Li, Z.; Cheng, W.; Dai, X.; Yang, K.; Zhang, H.; Zhang, Z.; Zhang, H. Exosome-like nanovesicles derived from *Phellinus linteus* inhibit Mical2 expression through cross-kingdom regulation and inhibit ultraviolet-induced skin aging. *J. Nanobiotechnol.* **2022**, *20*, 455. [CrossRef] [PubMed]
6. Sriwastva, M.K.; Deng, Z.B.; Wang, B.; Teng, Y.; Kumar, A.; Sundaram, K.; Mu, J.; Lei, C.; Dryden, G.W.; Xu, F. Exosome-like nanoparticles from Mulberry bark prevent DSS-induced colitis via the AhR/COPS8 pathway. *EMBO Rep.* **2022**, *23*, e53365. [CrossRef] [PubMed]
7. Chen, X.; Zhou, Y.; Yu, J. Exosome-like nanoparticles from ginger rhizomes inhibited NLRP3 inflammasome activation. *Mol. Pharm.* **2019**, *16*, 2690–2699. [CrossRef]

8. Perut, F.; Roncuzzi, L.; Avnet, S.; Massa, A.; Zini, N.; Sabbadini, S.; Giampieri, F.; Mezzetti, B.; Baldini, N. Strawberry-derived exosome-like nanoparticles prevent oxidative stress in human mesenchymal stromal cells. *Biomolecules* **2021**, *11*, 87. [[CrossRef](#)]
9. Li, D.; Yao, X.; Yue, J.; Fang, Y.; Cao, G.; Midgley, A.C.; Nishinari, K.; Yang, Y. Advances in Bioactivity of MicroRNAs of Plant-Derived Exosome-Like Nanoparticles and Milk-Derived Extracellular Vesicles. *J. Agric. Food Chem.* **2022**, *70*, 6285–6299. [[CrossRef](#)]
10. Zhang, M.; Viennois, E.; Prasad, M.; Zhang, Y.; Wang, L.; Zhang, Z.; Han, M.K.; Xiao, B.; Xu, C.; Srinivasan, S. Edible ginger-derived nanoparticles: A novel therapeutic approach for the prevention and treatment of inflammatory bowel disease and colitis-associated cancer. *Biomaterials* **2016**, *101*, 321–340. [[CrossRef](#)]
11. Munir, J.; Lee, M.; Ryu, S. Exosomes in food: Health benefits and clinical relevance in diseases. *Adv. Nutr.* **2020**, *11*, 687–696. [[CrossRef](#)] [[PubMed](#)]
12. Riso, P.; Klimis-Zacas, D.; Del Bo', C.; Martini, D.; Campolo, J.; Vendrame, S.; Møller, P.; Loft, S.; De Maria, R.; Porrini, M. Effect of a wild blueberry (*Vaccinium angustifolium*) drink intervention on markers of oxidative stress, inflammation and endothelial function in humans with cardiovascular risk factors. *Eur. J. Nutr.* **2013**, *52*, 949–961. [[CrossRef](#)] [[PubMed](#)]
13. De Robertis, M.; Sarra, A.; D'oria, V.; Mura, F.; Bordi, F.; Postorino, P.; Fratantonio, D. Blueberry-derived exosome-like nanoparticles counter the response to TNF- α -Induced change on gene expression in EA. hy926 cells. *Biomolecules* **2020**, *10*, 742. [[CrossRef](#)] [[PubMed](#)]
14. Zhao, W.-J.; Bian, Y.-P.; Wang, Q.-H.; Yin, F.; Yin, L.; Zhang, Y.-L.; Liu, J.-H. Blueberry-derived exosomes-like nanoparticles ameliorate nonalcoholic fatty liver disease by attenuating mitochondrial oxidative stress. *Acta Pharmacol. Sin.* **2022**, *43*, 645–658. [[CrossRef](#)]
15. Leng, Y.; Yang, L.; Pan, S.; Zhan, L.; Yuan, F. Characterization of blueberry exosome-like nanoparticles and miRNAs with potential cross-kingdom human gene targets. *Food Sci. Human Wellness* **2023**, *13*. [[CrossRef](#)]
16. Quan, S.-Y.; Nan, X.-M.; Wang, K.; Zhao, Y.-G.; Jiang, L.-S.; Yao, J.-H.; Xiong, B.-H. Replacement of forage fiber with non-forage fiber sources in dairy cow diets changes milk extracellular vesicle-miRNA expression. *Food Funct.* **2020**, *11*, 2154–2162. [[CrossRef](#)]
17. Kyung, K.Y.; Lee, Y.-H.; Sang-Woo, L. Anti-inflammatory Properties of Ginseng-Derived Exosome-like Nanoparticles in LPS-induced RAW264.7. *Res. Sq.* **2023**. [[CrossRef](#)]
18. Bruno, S.P.; Paolini, A.; D'Oria, V.; Sarra, A.; Sennato, S.; Bordi, F.; Masotti, A. Extracellular vesicles derived from citrus sinensis modulate inflammatory genes and tight junctions in a human model of intestinal epithelium. *Front. Nutr.* **2021**, *8*, 778998. [[CrossRef](#)]
19. Sánchez-López, C.M.; Manzaneque-López, M.C.; Pérez-Bermúdez, P.; Soler, C.; Marcilla, A. Characterization and bioactivity of extracellular vesicles isolated from pomegranate. *Food Funct.* **2022**, *13*, 12870–12882. [[CrossRef](#)]
20. Saliba, A.S.M.C.; de Oliveira Sartori, A.G.; Batista, P.S.; do Amaral, J.E.P.G.; da Silva, N.O.; Ikegaki, M.; Rosalen, P.L.; de Alencar, S.M. Simulated gastrointestinal digestion/Caco-2 cell transport: Effects on biological activities and toxicity of a Brazilian propolis. *Food Chem.* **2023**, *403*, 134330. [[CrossRef](#)]
21. Li, H.; Li, J.; Liu, L.; Zhang, Y.; Luo, Y.; Zhang, X.; Yang, P.; Zhang, M.; Yu, W.; Qu, S. Elucidation of the intestinal absorption mechanism of celastrol using the Caco-2 cell transwell model. *Planta Med.* **2016**, *82*, 1202–1207. [[CrossRef](#)] [[PubMed](#)]
22. KL, L. Analysis of relative gene expression data using real-time quantitative PCR and the 2- $\Delta\Delta$ CT method. *Methods* **2001**, *25*, 402–408.
23. Li, X.; Liang, Z.; Du, J.; Wang, Z.; Mei, S.; Li, Z.; Zhao, Y.; Zhao, D.; Ma, Y.; Ye, J. Herbal decoctosome is a novel form of medicine. *Sci. China Life Sci.* **2019**, *62*, 333–348. [[CrossRef](#)]
24. Shen, L.; Ma, J.; Yang, Y.; Liao, T.; Wang, J.; Chen, L.; Zhang, S.; Zhao, Y.; Niu, L.; Hao, X. Cooked pork-derived exosome nanovesicles mediate metabolic disorder—microRNA could be the culprit. *J. Nanobiotechnol.* **2023**, *21*, 83. [[CrossRef](#)] [[PubMed](#)]
25. Kantarcioğlu, M.; Yıldırım, G.; Oktar, P.A.; Yanbakan, S.; Özer, Z.B.; Sarıca, D.Y.; Taşdelen, S.; Bayrak, E.; Balı, D.F.A.; Öztürk, S. Coffee-Derived Exosome-Like Nanoparticles: Are They the Secret Heroes? *Turk. J. Gastroenterol.* **2023**, *34*, 161–169. [[CrossRef](#)] [[PubMed](#)]
26. Zhou, Z.; Li, X.; Liu, J.; Dong, L.; Chen, Q.; Liu, J.; Kong, H.; Zhang, Q.; Qi, X.; Hou, D. Honeysuckle-encoded atypical microRNA2911 directly targets influenza A viruses. *Cell Res.* **2015**, *25*, 39–49. [[CrossRef](#)]
27. Zand Karimi, H.; Baldrich, P.; Rutter, B.D.; Borniego, L.; Zajt, K.K.; Meyers, B.C.; Innes, R.W. Arabidopsis apoplasmic fluid contains sRNA-and circular RNA–protein complexes that are located outside extracellular vesicles. *Plant Cell* **2022**, *34*, 1863–1881. [[CrossRef](#)]
28. Jeyaram, A.; Jay, S.M. Preservation and storage stability of extracellular vesicles for therapeutic applications. *AAPS J.* **2018**, *20*, 1. [[CrossRef](#)]
29. Théry, C.; Witwer, K.W.; Aikawa, E.; Alcaraz, M.J.; Anderson, J.D.; Andriantsitohaina, R.; Antoniou, A.; Arab, T.; Archer, F.; Atkin-Smith, G.K. Minimal information for studies of extracellular vesicles 2018 (MISEV2018): A position statement of the International Society for Extracellular Vesicles and update of the MISEV2014 guidelines. *J. Extracell. Vesicles* **2018**, *7*, 1535750. [[CrossRef](#)]
30. Cao, M.; Yan, H.; Han, X.; Weng, L.; Wei, Q.; Sun, X.; Lu, W.; Wei, Q.; Ye, J.; Cai, X. Ginseng-derived nanoparticles alter macrophage polarization to inhibit melanoma growth. *J. Immunother. Cancer* **2019**, *7*, 326. [[CrossRef](#)]

31. Maroto, R.; Zhao, Y.; Jamaluddin, M.; Popov, V.L.; Wang, H.; Kalubowilage, M.; Zhang, Y.; Luisi, J.; Sun, H.; Culbertson, C.T. Effects of storage temperature on airway exosome integrity for diagnostic and functional analyses. *J. Extracell. Vesicles* **2017**, *6*, 1359478. [[CrossRef](#)] [[PubMed](#)]
32. Cheng, Y.; Zeng, Q.; Han, Q.; Xia, W. Effect of pH, temperature and freezing-thawing on quantity changes and cellular uptake of exosomes. *Protein Cell* **2019**, *10*, 295–299. [[CrossRef](#)] [[PubMed](#)]
33. Yuan, F.; Li, Y.-M.; Wang, Z. Preserving extracellular vesicles for biomedical applications: Consideration of storage stability before and after isolation. *Drug Deliv.* **2021**, *28*, 1501–1509. [[CrossRef](#)]
34. Xu, F.; Mu, J.; Teng, Y.; Zhang, X.; Sundaram, K.; Sriwastva, M.K.; Kumar, A.; Lei, C.; Zhang, L.; Liu, Q.M. Restoring Oat Nanoparticles Mediated Brain Memory Function of Mice Fed Alcohol by Sorting Inflammatory Dectin-1 Complex Into Microglial Exosomes. *Small* **2022**, *18*, 2105385. [[CrossRef](#)] [[PubMed](#)]
35. Li, D.; Cao, G.; Yao, X.; Yang, Y.; Yang, D.; Liu, N.; Yuan, Y.; Nishinari, K.; Yang, X. Tartary buckwheat-derived exosome-like nanovesicles against starch digestion and their interaction mechanism. *Food Hydrocoll.* **2023**, *141*, 108739. [[CrossRef](#)]
36. Yin, L.; Yan, L.; Yu, Q.; Wang, J.; Liu, C.; Wang, L.; Zheng, L. Characterization of the microRNA profile of ginger exosome-like nanoparticles and their anti-inflammatory effects in intestinal Caco-2 Cells. *J. Agric. Food Chem.* **2022**, *70*, 4725–4734. [[CrossRef](#)] [[PubMed](#)]
37. Liu, C.; Yan, X.; Zhang, Y.; Yang, M.; Ma, Y.; Zhang, Y.; Xu, Q.; Tu, K.; Zhang, M. Oral administration of turmeric-derived exosome-like nanovesicles with anti-inflammatory and pro-resolving bioactions for murine colitis therapy. *J. Nanobiotechnol.* **2022**, *20*, 206. [[CrossRef](#)] [[PubMed](#)]
38. Niu, G.; Jian, T.; Gai, Y.; Chen, J. Microbiome and plant-derived vesicles that serve as therapeutic agents and delivery carriers to regulate metabolic syndrome. *Adv. Drug Deliv. Rev.* **2023**, *196*, 114774. [[CrossRef](#)]
39. Karamanidou, T.; Tsouknidas, A. Plant-derived extracellular vesicles as therapeutic nanocarriers. *Int. J. Mol. Sci.* **2021**, *23*, 191. [[CrossRef](#)]
40. Garaeva, L.; Kamyshinsky, R.; Kil, Y.; Varfolomeeva, E.; Verlov, N.; Komarova, E.; Garmay, Y.; Landa, S.; Burdakov, V.; Myasnikov, A. Delivery of functional exogenous proteins by plant-derived vesicles to human cells in vitro. *Sci. Rep.* **2021**, *11*, 6489. [[CrossRef](#)]
41. Nemidkanam, V.; Chaichanawongsaroj, N. Characterizing Kaempferia parviflora extracellular vesicles, a nanomedicine candidate. *PLoS ONE* **2022**, *17*, e0262884. [[CrossRef](#)] [[PubMed](#)]
42. Nguyen, T.N.-G.; Pham, C.V.; Chowdhury, R.; Patel, S.; Jaysawal, S.K.; Hou, Y.; Xu, H.; Jia, L.; Duan, A.; Tran, P.H.-L. Development of Blueberry-Derived Extracellular Nanovesicles for Immunomodulatory Therapy. *Pharmaceutics*. **2023**, *15*, 2115. [[CrossRef](#)] [[PubMed](#)]
43. Fang, Y.; Wang, Z.; Zhang, S.; Peng, Q.; Liu, X. Characterization and proteome analysis of the extracellular vesicles of *Phytophthora capsici*. *J. Proteomics*. **2021**, *238*, 104137. [[CrossRef](#)] [[PubMed](#)]

Disclaimer/Publisher's Note: The statements, opinions and data contained in all publications are solely those of the individual author(s) and contributor(s) and not of MDPI and/or the editor(s). MDPI and/or the editor(s) disclaim responsibility for any injury to people or property resulting from any ideas, methods, instructions or products referred to in the content.